



Spectrometric assay for horseradish peroxidase activity based on the linkage of conjugated system formed by oxidative decarboxylation

Masaki Yamaguchi, Shingo Sato *

Department of Biochemical Engineering, Graduate School of Science and Engineering, Yamagata University, Jonan 4-3-16, Yonezawa-shi, Yamagata 992-8510, Japan

ARTICLE INFO

Article history:

Received 18 April 2016

Received in revised form 25 October 2016

Accepted 12 November 2016

Available online 13 November 2016

Keywords:

Carthamin-precursor model

Oxidative decarboxylation

Horseradish peroxidase

Spectrocolorimetry

Spectrofluorometry

ABSTRACT

Horseradish peroxidase (HRP)-catalyzed oxidation of 2,2-bis[3-acetylfillicinic acid-5-yl]acetic acid (BAFA, **4**) produces Dehydro-3,3'-diacetyl-5,5'-methylene-difillicinic acid (DDMF, **3**). A new photometric hydrogen donor (**4**) for peroxidase (POD)-catalyzed oxidation was demonstrated to be potentially useful for spectrophotometric and spectrofluorometric determination of HRP. Our developed colorimetric (absorption at 483 nm) and fluorometric (emission at 529 nm) systems both gave a linear calibration curve for HRP ($y = 0.0025x + 0.0237$; $R^2 = 0.9997$, and $y = 0.241x + 3.194$; $R^2 = 0.9914$, respectively) in the same concentration range of 9.1×10^{-8} – 1.1×10^{-6} nmol/L. The calculated K_m and V_{max} values of 5.10×10^{-4} M and 5.13×10^{-6} M/min, respectively. The results indicate that the quantification of HRP using BAFA **4** as hydrogen donor is possible.

© 2016 Elsevier B.V. All rights reserved.

1. Introduction

The spectrometric determination of peroxidase (POD) using a chromogenic compound is one of the most important analytical methods and has widespread applications in clinical and environmental chemistry. Horseradish peroxidase (HRP) is heme peroxidase [1] and catalyzes a variety of oxidative transformations of organic and inorganic substrates [2,3]. Peroxidases such as HRP are frequently used as markers or labels in enzyme-linked assays for biological molecules and other analytes of interest, e.g., drugs, hormones, steroids, and cancer markers [4–12]. Detection of these enzymes can be achieved by the use of substrates that produce a detectable product. Chromogenic compounds such as *o*-phenylenediamine [13,14] 2,2'-azino-bis(3-ethylbenzothiazoline-6-sulfonic acid) (ABTS) [15], tetramethylbenzidine [16] and diaminodiphenylmethane [17] produce a colored reaction product, and fluorogenic substrates produce fluorescent products [4–12]. These methods offer a safe, convenient, and sensitive means to provide a quantitative measurement of the amount of enzyme or an enzyme-labeled analyte in a sample.

The color of the petals of safflower (*Carthamus tinctorius* L.) gradually changes from yellow to red. The red pigment is referred to as carthamin (**1**) [18] and has been used for a long time as a dye stuff, rouge, and food colorant. Red pigment **1** is formed by POD-catalyzed oxidative decarboxylation of one of the yellow pigments in safflower petal, which is referred to as carthamin precursor (**2**) [20,21] (Scheme 1). This remarkable color change led us to assume that yellow dye **2** could be

used as a visual detection reagent of POD. However, both pigments **1** and **2** are unstable and are present only in small quantities in safflower petals; moreover, **2** is readily oxidized to **1**. Because of their complexity, the synthesis of both **1** and **2** has not yet been achieved. On the basis of the experience in synthesis [21,22], we here design more stable, readily synthesizable, and water-soluble model compounds (DDMF **3** [19] and BAFA **4** [20]) for the detection of POD, in which the hydroxyl and glucosyl residues of **1** and **2** are replaced by methyl groups and the cinnamoyl moieties are replaced by acetyl groups (Scheme 1). Model compounds **3** and **4** take over the linkage of the conjugated system due to the sp^2 -carbon formed by oxidative decarboxylation from natural dyes. This structure and oxidation reaction mechanism are new and differ from those of the commercially available reagents used for POD detection. We here describe a spectrometric method for the determination of HRP activity using BAFA **4** as a hydrogen donor for HRP.

2. Experiment

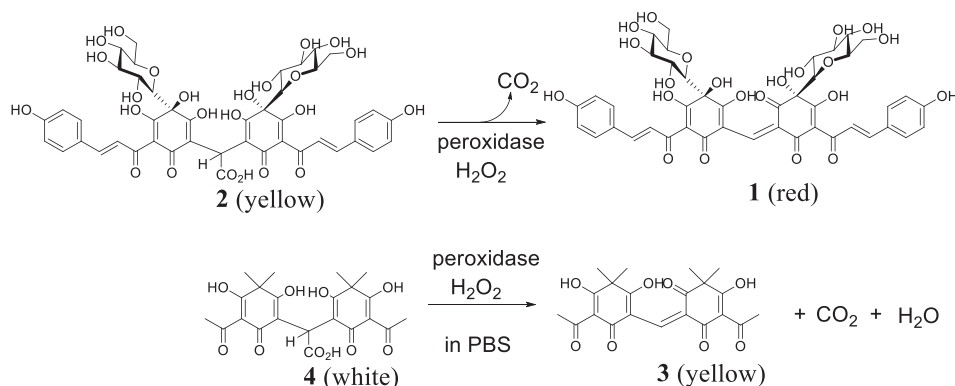
2.1. Synthesis

2.1.1. Reagents and Apparatus

All solvents used in this synthesis were commercial products. Reactions were monitored by TLC on 0.25-mm silica gel F254 plates (E. Merck, Japan). UV light irradiation (254 and 365 nm), a 5% ethanolic solution of ferric chloride, and a 7% ethanolic solution of phosphomolybdic acid with heat were used as coloring agents. For the separation and purification of the reaction products, flash column chromatography on silica gel (40–50 μ m, Kanto Reagents Co. Ltd., Japan, silica-gel 60) was performed. Melting points were determined using

* Corresponding author.

E-mail address: shingo-s@yz.yamagata-u.ac.jp (S. Sato).



Scheme 1. Biosynthesis carthamin (1) by oxidative decarboxylation of its precursor yellow pigment (2) in safflower petals, and their model compounds (DDMF 3, BAFA 4).

an ASONE micro-melting point apparatus and are uncorrected. IR spectra were recorded on a Horiba FT-720 IR spectrometer using a KBr disk. NMR spectra were recorded on a JEOL ECX-500 spectrometer using Me₄Si as the internal standard. Mass spectral data were obtained by fast-atom bombardment (FAB) in a matrix of 3-nitrobenzyl alcohol (NBA), using a JEOL JMS-AX505HA instrument. High-resolution mass spectra (HRMS) were obtained under electro spray ionization (ESI) conditions on a JEOL JMS-T100LP.

2.1.2. Synthesis of 3 and 4

DDMF 3 and BAFA 4 were synthesized as shown in Scheme 2.

2.1.2.1. Synthesis of Dehydro-3,3'-bis(acetyl)-5,5'-methylenedifilicinic Acid (Dehydro-3,3'-diacetyl-5,5'-methylenedifilicinic acid (DDMF, 3)). To a stirred suspension solution of 2-acetyl-3,5-dihydroxy-4,4-dimethyl-2,5-cyclohexadien-1-one (5 [23,24], 100 mg) in triethyl orthoformate (3 mL), 60% NaH (245 mg, 12 equiv) was added portion wise and the mixture was vigorously stirred at room temperature for 2.5 h. After complete consumption of 5 as monitored by TLC, the reaction mixture was poured into an ice-cold 1 M HCl solution (30 mL) and extracted two times with EtOAc. After removal of the solvent, the residue was purified by silica-gel column chromatography (toluene/EtOAc/AcOH = 6:1:0.1) and recrystallized from benzene to afford 3 (74.7 mg, 78%) as yellow prisms.

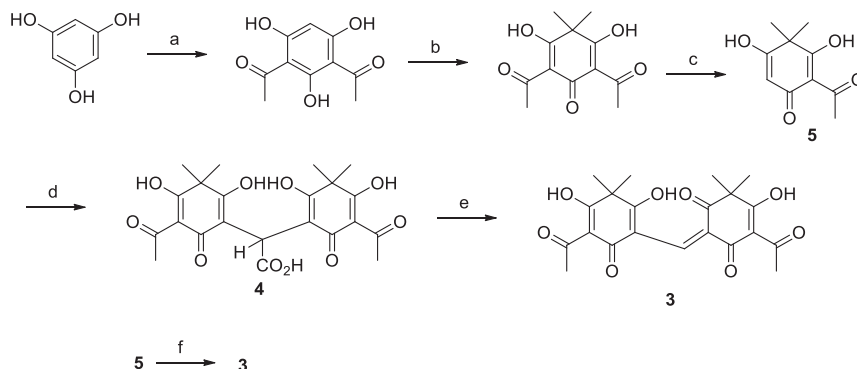
2.1.2.1.1. Data of 3. Yellow prisms. Mp = 173.0–174.5 °C (lit [19] 173.0–174.5 °C). IR ν (KBr) 3315, 2983, 2945, 2879, 1682, 1651, 1540 cm⁻¹. ¹H NMR (pyrine-d₅) δ 1.66 (12H, s, —CH₃ × 4), 2.69 (6H, s, —Ac × 2), 9.14 (1H, s, —CH=). ¹³C NMR (pyrine-d₅) δ 23.00 (CH₃ × 4), 28.73 (Ac × 2), 54.77 (quaternary C), 106.79, 112.89,

138.08, 184.08, 197.45, 200.95. FAB-MS (*m/z*) 403 (M + H)⁺. HRMS (ESI⁺) *m/z*: [M + Na]⁺ calcd. for C₂₁H₂₂NaO₈ 425.12124, found 425.12119. UV-vis λ_{\max} (EtOH) 482 nm; log ϵ 4.46.

2.1.2.2. Synthesis of 2,2-Bis[3-acetylfilicinic acid-5-yl]acetic Acid (BAFA 4). To a stirred solution of 5 (210 mg) in 1 M Na₂CO₃ aqueous solution (2 mL), glyoxylic acid (59 mg, 0.6 equiv) was added and the mixture was stirred at room temperature for 0.5 h. The reaction mixture was poured into an ice-cold 1 M HCl solution (30 mL) and extracted two times with EtOAc. After removal of the solvent, the residue was purified by silica-gel column chromatography (toluene/EtOAc/AcOH = 6:1:0.1) and recrystallized from benzene to afford 4 (164 mg, 73%) as white prisms.

2.1.2.2.1. Data of 4. White prisms. Mp = 103–105 °C (lit [21] 102–105 °C). IR ν (KBr) 3480, 2981, 2939, 2872, 1749, 1722, 1643, 1564, 1540 cm⁻¹. ¹H NMR (pyrine-d₅, 500 MHz) δ 1.61 and 1.72 (each 6H, s, CH₃ × 4), 2.71 (6H, s, Ac × 2), 6.84 (1H, s, >CH—). ¹³C NMR (pyrine-d₅) δ 24.40, 36.25, 28.24, 34.01 (>CH—), 51.34 (quaternary C), 104.87, 105.41, 175.31, 186.53, 189.52, 197.87, 198.23. FAB-MS (*m/z*) 449 (M + H)⁺. HRMS (ESI⁻) *m/z*: [M—H]⁻ calcd. for C₂₂H₂₃O₁₀ 447.12912, found 447.12950. UV-vis λ_{\max} (EtOH) 342 nm; log ϵ 4.25.

2.1.2.3. Acetylfilicinic Acid; 2-Acetyl-4,4-dimethylcyclohexan-1,3,5-trione (5) [24,25]. Colorless prisms. Mp = 108–109 °C. ¹H NMR (DMSO-d₆) δ 1.28 (6H, s, CH₃ × 2), 2.47 (3H, s, COCH₃), 5.43 (1H, s, olefinic H), 18.41 (1H, s, OH). ¹³C NMR (DMSO-d₆) δ 24.6 (CH₃), 28.3 (COCH₃), 48.7 (C4), 94.9 (C6), 105.2 (C2), 182.5 (C=O), 188.7, 196.7 and 200.5 (C1, 3, 5).



Reagents and conditions: a) BF₃·2AcOH, at 100 °C, 2 h, Y:84% b) MeI (4 eq), NaOMe (4 eq) in dried MeOH at 0 °C - r.t., 4 h, Y:78% c) 80% H₂SO₄, at 80 °C, 1 h, Y:89% d) glyoxylic acid (0.6 eq) in 1M Na₂CO₃ aq.soln at r.t., 0.5 h, Y:73% e) 0.25% KMnO₄ aq. soln / acetone (1:1.15), at r.t., 2 h, Y:30% f) 60% NaH (12 eq) in (EtO)₃CH, at r.t., 2.5 h, Y:78%

Scheme 2. Synthesis of 3 and 4.

2.2. Analysis

2.2.1. Reagents and Apparatus

The reagents used in analysis were commercial products: peroxidase from horseradish (Wako Pure Chemical Industries, Ltd., Osaka, Japan) with optimum pH 5.0–8.0 and activity 383 units/mg [5]; 30% H₂O₂ aqueous solution (Wako Pure Chemical Industries, Ltd.); anthracene (Sigma-Aldrich, St. Louis, MO, USA).

UV–vis absorption spectra were obtained using a Hitachi U-2010 UV–VIS spectrophotometer. Fluorescence spectra and quantum yield were measured using a Hitachi F-7000 fluorescence spectrophotometer. Excitation and emission wavelength band passes were set at 2 nm.

2.2.2. Preparation of Sample Solutions for UV–vis and Fluorescence Spectroscopy (Figs. 1–3, Tables 1 and 2)

Solutions of **3** and **4** with a concentration of 3.0×10^{-5} M were prepared in EtOH, MeOH, CHCl₃, acetone, and 0.01 M phosphate buffer solution (PBS) (pH 6.5), and were subjected to UV–vis and fluorescence measurements.

2.2.3. Determination of the Fluorescence Quantum Yield of **3** (Table 3) [25]

The fluorescence quantum yields for **3** in EtOH and MeOH were obtained by comparing the area of the emission spectrum for a reference sample with that for a solution of anthracene excited at the same wavelength. The fluorescence quantum yields were obtained from the following equation:

$$\Phi_{\text{sample}} = \Phi_{\text{standard}} \times \left(\frac{A_{\text{standard}}/A_{\text{sample}}}{n_{\text{sample}}^2/n_{\text{standard}}^2} \right) \times \left(\frac{\Sigma[F_{\text{sample}}]}{\Sigma[F_{\text{standard}}]} \right) \quad (1)$$

where A, F, $\Sigma[F]$ and n^2 denote absorbance, fluorescence intensity, the peak area of the fluorescence spectra, and refractive index of the used solvent, respectively. Here, anthracene was as a standard and its quantum yield (Φ_{standard}) in EtOH is 0.27 [25]. Since measurement of both sample **3** and standard (anthracene) was conducted with both the concentration of 3.0×10^{-5} mol/L using EtOH as a solvent, the term of the refractive index ($n_{\text{sample}}^2/n_{\text{standard}}^2$) was removed from the Eq. (1). Each data determined from the measurement; A_{standard} :0.136, A_{sample} :0.501, $\Sigma[F_{\text{sample}}]$:2636.4, $\Sigma[F_{\text{standard}}]$:21396 was introduced to Eq. (1).

$$\Phi_{\text{sample}} = 0.27 \times (0.136/0.501) \times (2636/21,396) = 9.0 \times 10^{-3}$$

The quantum yield of **3** in EtOH was determined to be 9.0×10^{-3} .

Next, each data measured in MeOH, A_{sample} :0.367, $\Sigma[F_{\text{sample}}]$: 5997.2, n_{sample} :1.3289, n_{standard} :1.3614 was introduced to Eq. (1).

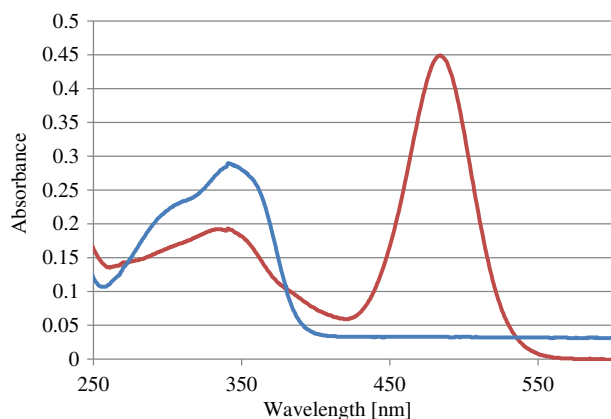


Fig. 1. UV–vis spectra of **3** and **4** in EtOH (both 1.6×10^{-5} M, –**3**, –**4**). (For interpretation of the references to color in this figure legend, the reader is referred to the web version of this article.)

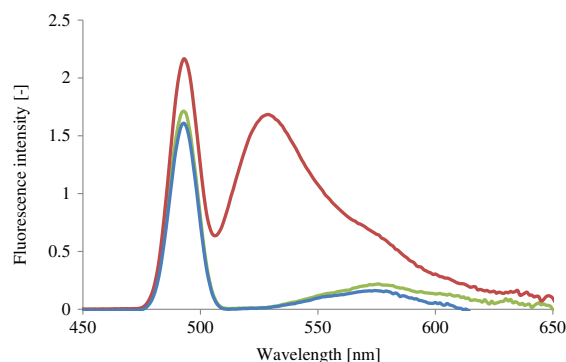


Fig. 2. Fluorescence spectra of **3** and **4** in EtOH (–EtOH, –**3**, –**4**, both 3.0×10^{-7} M). (For interpretation of the references to color in this figure legend, the reader is referred to the web version of this article.)

$$\Phi_{\text{sample}} = 0.27 \times (0.136/0.367) \times (5997.2/21,396) \times (1.3289^2/1.3614^2) = 2.7 \times 10^{-2}$$

The quantum yield of **3** in MeOH was determined to be 2.7×10^{-2} .

2.2.4. Examination of the Detection of HRP Using **4**

2.2.4.1. Absorbance at Different Concentrations of H₂O₂ in the Presence of HRP. Mixtures of 0.01 M PBS (4.5 mL, pH 6.5) of **4** (1.0 mg) with 0.01 M PBS (0.5 mL, pH 6.5) containing HRP (0.1 mg) were prepared, 20 μ L of 0.03, 0.3, 3.0, or 30% H₂O₂ aqueous solution was added, and the reactions were mixed. The resulting solutions were sampled at 10 min intervals for 60 min, diluted 10 times with EtOH, and subjected to UV–vis or fluorescence measurement.

2.2.4.2. Absorbance at Different Concentrations of PBS (pH 6.5) in the Presence of HRP. Substrate **4** (1.0 mg) was dissolved in 4.5 mL of H₂O and in 0.01, 0.05, 0.1, and 0.5 M PBS (pH 6.5). To each solution, 0.5 mL of a solution of the same concentration containing HRP (0.1 mg) and 20 μ L of 0.03% H₂O₂ was added, and the mixtures were stirred. After stirring for 1 h, the resulting solution was diluted 10 times with EtOH and subjected to UV–vis spectroscopy measurement. When 0.5 M PBS was used, the mixture was left to stand overnight to allow the resulting salts to precipitate, and the supernatant was subjected to analysis.

2.2.4.3. Absorbance at Different pH Values in the Presence of HRP and H₂O₂. Substrate **4** (1.0 mg) was dissolved in 4.5 mL of 0.01 M PBS of different pH (pH 5.0, 5.5, 6.0, 6.5, 7.0, 7.5, and 8.0). To each solution, 0.5 mL of a PBS of the same pH containing HRP (0.1 mg) and 20 μ L of 0.03% H₂O₂ were added and the mixtures were stirred. After diluting 10 times with EtOH, the ABS and fluorescence intensity of the resulting mixtures

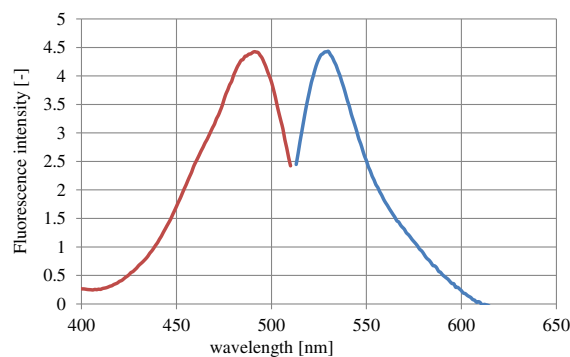


Fig. 3. Excitation and Emission spectra of **3** in EtOH (– excitation, – emission). (For interpretation of the references to color in this figure legend, the reader is referred to the web version of this article.)

Table 1

Visible absorption spectra of **3** in different solvents [CHCl₃, acetone, EtOH, MeOH, PBS (0.01 M, pH 6.5)].

Solvent	CHCl ₃	Acetone	EtOH	MeOH	PBS (0.01 M, pH 6.5)
λ_{\max} (nm)	–*	489	483	470	467
Absorbance (–)	–	0.135	0.740	0.356	0.310

* No absorption in a visible region.

were measured at 20 min intervals for 120 min at a wavelength of 482 nm and emission wavelength of 529 nm (excitation wavelength: 492 nm).

2.2.4.4. Measurement of the Detection Limit of HRP by Colorimetry and Fluorometry (Fig. 6). To 4.5 mL of a 0.01 M PBS (pH 6.0) containing **4** (1.0 mg), 0.5 mL of 0.01 M PBS (pH 6.0) containing concentrations of HRP in the range 8.98×10^{-2} –11.5 U/L with 2-fold dilution and 20 μ L of 0.03% aqueous H₂O₂ were added and the oxidation reaction was started. Each resulting solution was diluted 10 times with EtOH and subjected to colorimetric and fluorometric analyses.

2.2.4.5. Determination of K_m and V_{max} . EtOH solutions of **3** at the concentrations of 3.1×10^{-5} to 6.1×10^{-8} M with 2-fold dilution was prepared, their ABS was measured at 482 nm, and their calibration curve was determined. Next, 0.01 M PBS (pH 6.0) of **4** at concentrations from 1.1×10^{-3} to 1.7×10^{-5} M with 2-fold dilutions were prepared. To each, a PBS (1.5 mL) containing HRP at a concentration of 15.7 U/L and a 0.03% H₂O₂ aqueous solution (20 μ L) were added, and the oxidation reaction was performed for 5 min. The resulting mixtures were diluted 10 times with EtOH and the ABS was measured at 1 min intervals.

3. Results and Discussion

3.1. Synthesis [19–24]

The synthesis of **3** and **4** was conducted as shown in Scheme 2. Compounds **3** (yellow) and **4** (white) were afforded via a four-step sequence in 45 and 43% overall yields, respectively. On the synthesis of **3** by oxidation of **4** using metal oxide such as KMnO₄, the reaction proceeded, however gave a mixture of the complex products including **3**. In the oxidation using H₂O₂/peroxidase, water-solubility of **4** was poor under the synthetic conditions. Dimerization of acetylflilicinic acid **5** using triethyl orthoformate in the presence of NaH was smoothly proceeded and gave **3** as an only product. Both are recrystallizable from benzene, and the resulting crystals are stable and can be stored at room temperature for long periods.

3.2. Analysis

The UV–vis spectra of **3** and **4** in EtOH showed a maximum absorption at 482 nm (log ϵ 4.46) and 342 nm (log ϵ 4.25), respectively and no overlapping signals (Fig. 1). Whereas **4** exhibited no fluorescence, **3** emitted a weak yellowish green fluorescence in EtOH (Figs. 2 and 3). The UV–vis and fluorescence spectra of **3** were measured in different solvents [EtOH, MeOH, CHCl₃, and PBS, (pH 6.5)], and the maximum absorbance and fluorescence intensity were observed in EtOH and MeOH, respectively (Tables 1 and 2). The maximum emission wavelength of **3**

Table 2

Fluorescence spectra of **3** in different solvents [CHCl₃, acetone, EtOH, MeOH, PBS (0.01 M, pH 6.5)].

Solvent	CHCl ₃	Acetone	EtOH	MeOH	PBS (0.01 M, pH 6.5)
λ_{em} (nm)	493	495	530	527	529
Fluorescence intensity (–)	56.94	12.33	170.1	834.6	47.14

Table 3

The fluorescence quantum yield (Φ) of **3** in EtOH and MeOH.

Solvent	Fluorescence quantum yield (Φ)
EtOH	9.0×10^{-3}
MeOH	2.7×10^{-2}

in EtOH and MeOH was 529 nm and the quantum yield (Φ) was determined to be 9.0×10^{-3} and 2.7×10^{-2} , respectively (Table 3). Because the use of **4** was proposed for the color- and fluorometric determination of HRP, HRP quantification methods using this model compound were evaluated.

In order to determine the optimum conditions for UV–vis and fluorescence measurements, the HRP-catalyzed oxidative decarboxylation reaction of **4** was examined. In the absence of HRP, the oxidation of **4** (1 mg) with 30% hydrogen peroxide (H₂O₂) aqueous solution (20 μ L) in 0.1 M PBS (pH 6.5) did not proceed and **4** was stable for at least 8 h. In the presence of HRP (0.1 mg), the time-course of the ABS at 482 nm was measured at the presence of 20 μ L of the concentrations of 0.03, 0.3, 3, and 30% H₂O₂ under the same oxidation conditions (Fig. 4). When the concentration of H₂O₂ was 0.03%, the highest ABS (1.2) was observed, which remained constant for 30 min. When the concentration of H₂O₂ was over 0.3%, formation of the unknown oxidation products is possible. When the adding concentration of H₂O₂ was 0.003%, the ABS decreased to 1.0 over 1 h. Thus, the optimum H₂O₂ concentration and reaction time were determined to be 0.03% and 1 h, respectively. Next, the optimum concentration and pH of the PBS were examined. The ABS of **4** at 482 nm was measured for solutions with increasing concentrations of PBS from 0 (H₂O) to 0.01, 0.05, 0.1, and 0.5 M, in the presence of 0.03% H₂O₂ (20 μ L) and HRP (0.1 mg) (Table 4). The measurement was carried out after 10-fold dilution with EtOH. The ABS was higher at higher concentrations of PBS (pH 6.5). However, because the salt was precipitated by the addition of EtOH at concentrations >0.05 M, the optimum concentration of PBS was determined to be 0.01 M. Thus, the ABS at 482 nm of each reaction mixture in 0.01 M PBS (pH 5.0–8.0) in the presence of HRP (0.1 mg) and 0.03% H₂O₂ (20 μ L) was measured (Fig. 5), and a maximum ABS of 1.1 was recorded at pH 6.0. Analysis of the time-course of the ABS at each pH shows that the maximum ABS at pH 6.0 was maintained for 80 min. Thus, the optimum pH was determined to be 6.0. In the HRP-catalyzed oxidative coupling reaction of pyrocatechol and aniline, the maximum ABS was from pH 6.5 to 8.5 in the pH region of 4.5–8.5 and the optimum pH chosen was 7.0 because pyrocatechol is acidic and aniline is basic [1]. Our sample **3** and **4** are acidic and unstable in basicity. Next, the ABS was measured in the concentration range of 8.98×10^{-2} –11.5 U/L HRP with 2-fold dilution,

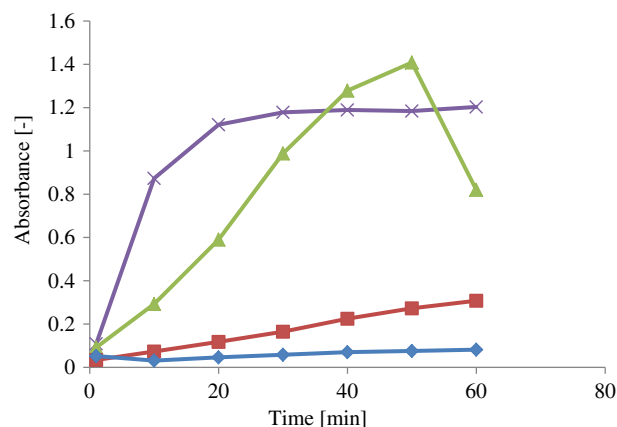


Fig. 4. Time-dependent absorbance of **4** (1.0 mg) at 480 nm in 5 mL of a 0.1 M PBS (pH 6.5) in the presence of 20 μ L of 0.03–30% H₂O₂ solutions (–0.03%, –0.30%, –3.00%, –30%) and HRP (0.1 mg). (For interpretation of the references to color in this figure legend, the reader is referred to the web version of this article.)

Table 4

Absorption spectra on the oxidation reaction of **4** in H₂O and 0.01–0.5 M PBS (pH 6.5) in the presence of 0.03% H₂O₂ solution (20 μ L) and HRP (0.1 mg).

Solvents	H ₂ O	0.01 M	0.05 M	0.1 M	0.5 M
Absorbance [–]	0.446	1.024	1.038	1.086	1.244

under the optimum conditions. The relationship between the ABS and the concentration of HRP 1.4–11.5 U/L was linear ($y = 0.0025x + 0.0237$, $R^2 = 0.9997$) and can be used as a calibration curve. The value of 1.4 U/L represents the cross point and the limit of this quantification method [1]. The relation between fluorescence intensity and concentration of HRP (excitation: 482 nm; emission: 529 nm) was measured by fluorometry in a manner similar to that above-described for the colorimetric assay. Similarly to the colorimetric data, a linear relationship was observed in the concentration range from 1.4 to 11.5 U/L ($y = 0.241x + 3.1942$, $R^2 = 0.9914$), which could also be used as a calibration curve. Although the colorimetric and fluorometric measurements were performed in the same HRP concentration range 1.4–11.5 U/L (Fig. 6). The limit of this quantification method (detection limit for HRP), 1.4 U/L (9.1×10^{-14} mol/mL) is analogous to that using tyramine (2.3×10^{-14} mol/mL), homovanillic acid (1.1×10^{-13} mol/mL), and *N,N'*-dicyanomethyl *o*-phenylenediamine (1.0×10^{-13} mol/mL) as fluorescent substrates [4], and pyrocatechol-aniline (1.42×10^{-13} mol/mL) and phenol-aminoantipyridine (2.31×10^{-13} mol/mL) as colored substrates [1], but higher than that using *p*-hydroxyphenylpropionic acid (6.5×10^{-16} mol/mL), tyrosol (1.3×10^{-15} mol/mL), and amino aluminum phthalocyanine (6.0×10^{-15} mol/mL) [4].

For the determination of the Michaelis-Menten and Lineweaver-Burk plots, the calibration curve of the ABS at 483 nm vs. HRP concentration [0.06–31.0 μ M in 0.01 M PBS (pH 6.0)] was prepared. The calibration curve was calculated as $y = 0.0485x + 0.0027$, and the correlation coefficient (R^2) was 0.9999. Because of its high linearity, this equation could be used for the determination of the Michaelis-Menten plot and of the Lineweaver-Burk plot. The K_m and V_{max} values were calculated to be 5.10×10^{-4} M and 5.13×10^{-6} M/min, respectively, using the equation: $y = 99.572x + 0.1951$, derived from the Lineweaver-Burk plot. As compared with the K_m (1.25×10^{-2} M) and the V_{max} (1.22×10^{-5} M/min) of the HRP-catalyzed oxidative coupling reaction of pyrocatechol and aniline [1], the affinity of the substrate for HRP was 24.5-fold higher and the maximum reaction rate was 2.38-fold slower. This shows that the catalytic ability of HRP is low for the abstraction of labile carboxylic and enol proton atoms of **4**. However, taking into account the detection limit for HRP and the affinity of **4** for HRP, the HRP activity for **4** is adequate for practical applications.

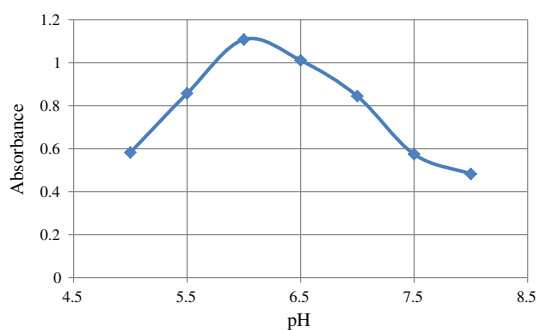


Fig. 5. Effects of the pH on the HRP-catalyzed oxidation reactions of **4** in a 0.01 M PBS in the presence of a 0.03% H₂O₂ solution.

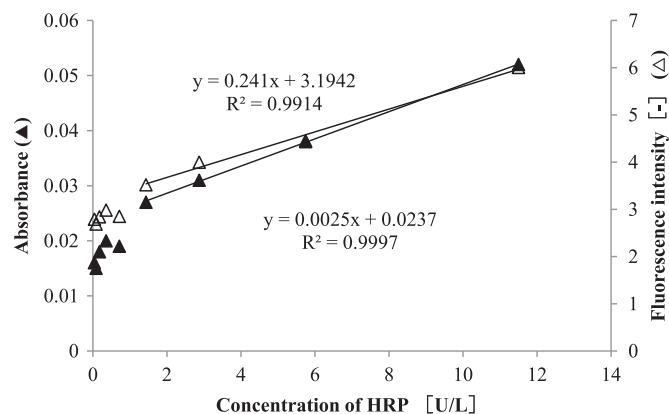


Fig. 6. Calibration curve of the absorbance at 483 nm and the fluorescence intensity at 582 nm vs. concentration of HRP (0–11.5 U/L).

4. Conclusion

The HRP-catalyzed oxidative decarboxylation of BAFA **4** proceeded smoothly to form a yellow DDMF **3** in the presence of 0.03% H₂O₂ (20 μ L) in 0.01 M PBS (pH 6.0, 5 mL) without exposure to light. Nonfluorescent BAFA **4** was converted into a fluorescent DDMF **3** with fluorescence quantum yield of 0.027 and emission wavelength at 529 nm. The color- and fluorometric quantification of HRP using BAFA **4** as hydrogen donor is demonstrated. Kinetic parameters, K_m (1.25×10^{-2} M) and V_{max} (1.22×10^{-5} M/min) are suggested that BAFA **4** is an appropriate hydrogen donor for the HRP spectrometric assay. The color- and fluorometric quantification of HRP using **4** as hydrogen donor is demonstrated. Many substrates for HRP are coupling products of the two components such as 2,2'-dihydrodiphenyl derivatives, which are one component is subjected to HRP-catalyzed oxidation with H₂O₂ and coupled with another component [4a]. Our developed substrate, BAFA **4** is one component and subjected to the HRP-catalyzed oxidative decarboxylation with H₂O₂ to give colored and fluorogenic DDMF **3**. Thus this reaction is simple and difficult to be influenced. For practical applications, further studies using vital fluids such as blood are required.

Conflict of Interest

The authors declare no conflict of interest.

Acknowledgement

The authors wish to thank Professor Bunpei Hatano for HRMS measurements and Mr. Koya Maeda and Mr. Kota Sasaki for their technical assistance.

References

- [1] A. Molaei Rad, H. Ghourchian, A.A. Moosavi-Movahedi, J. Hong, K. Nazari, *Anal. Biochem.* 362 (2007) 38–43.
- [2] P. Singh, R. Prakash, K. Shah, *Talanta* 97 (2012) 204–210.
- [3] K. Yoshida, P. Kaothien, T. Matsui, A. Kawaoka, A. Shinmyo, *Appl. Microbiol. Biotechnol.* 60 (2003) 665–670.
- [4] (a) H. Akhavan-Tafti, R. deSilva, R. Eickholt, R. Handley, M. Mazelis, M. Sandison, *Talanta* 60 (2003) 345–354; (b) K. Zaitzu, Y. Okura, *Anal. Biochem.* 109 (1980) 109; (c) K. Matsuoka, M. Maeda, A. Tsuji, *Chem. Pharm. Bull.* 27 (10) (1979) 2345.
- [5] M. Zhu, X. Huang, H. Shen, *Talanta* 53 (2001) 927–935.
- [6] Q.T. Smith, C.H. Yang, *Proc. Soc. Exp. Biol. Med.* 175 (1975) 468.
- [7] H.B. Dunford, J. Everse, K.E. Everse, M.B. Grisham (Eds.), *Peroxidase in Chemistry and Biology*, vol. II, CRC Press, Boca Raton 1991, pp. 1–24.
- [8] G.G. Guilbault, *Handbook of Enzymatic Methods of Analysis*, Marcel Dekker, Inc., New York and Basel, 1976.
- [9] P.M. Iunitskii, R.A.V. Sitdikov, E. Kurochkin, *Anal. Chim. Acta* 261 (1992) 45.
- [10] W.D. Geoghegan, in: T.T. Ngo, H.P. Howard (Eds.), *Enzyme-mediated Immunoassay* 1985, pp. 451–465 (New York, NY).

- [11] M. Schaferling, D.B.M. Grogel, S. Schreml, *Microchim. Acta* 174 (2011) 1–18.
- [12] S. Watanabe, Y. Sakamoto, M. Morikawa, R. Okada, T. Miura, E. Ito, *PLoS One* 6 (8) (2011), e22955.
- [13] P.J. Tarcha, V.P. Chu, D. Whittern, *Anal. Biochem.* 165 (1987) 230–233.
- [14] S. Fornera, P. Walde, *Anal. Biochem.* 407 (2010) 293–295.
- [15] D.I. Matelitz, A.N. Eryomin, D.O. Sviridov, V.S. Kamyshnikov, *Biochem. Mosc.* 66 (5) (2001) 505–514.
- [16] P.D. Josephy, T. Eling, R.P. Mason, *J. Biol. Chem.* 257 (7) (1982) 3669–3675.
- [17] M. Mizoguchi, M. Shiga, K. Sasamoto, *Chem. Pharm. Bull.* 41 (3) (1993) 620–623.
- [18] (a) C. Kuroda, *Nippon Kagaku Kaishi* 51 (1930) 237;
(b) C. Kuroda, *J. Chem. Soc.* (1930) 752;
(c) T.R. Seshadri, R.S. Thakur, *Curr. Sci.* 29 (2) (1960) 54;
(d) H. Obara, J. Onodera, *Chem. Lett.* (1979) 201–204;
(e) Y. Takahashi, N. Miyasaka, S. Tasaka, I. Miura, S. Urano, M. Ikura, K. Hikichi, T. Matsumoto, M. Wada, *Tetrahedron Lett.* 23 (1982) 5163.
- [19] H. Obara, J. Onodera, S. Abe, T. Saito, *Bull. Chem. Soc. Jpn.* 53 (1980) 289–290.
- [20] T. Kumazawa, S. Sato, D. Kanenari, A. kunimatsu, R. Hirose, S. Matsuba, H. Obara, M. Suzuki, N. Sato, J. Onodera, *Chem. Lett.* (1994) 2343–2344.
- [21] T. Kumazawa, Y. Amano, T. Haga, S. Matsuba, S. Sato, K. Kawamoto, J. Onodera, *Chem. Lett.* (1995) 625–626.
- [22] S. Sato, T. Kumazawa, H. Watanabe, K. Takayanagi, S. Matsuba, J. Onodera, H. Obara, K. Furuhashi, *Chem. Lett.* (2001) 1318–1319.
- [23] S. Sato, T. Kusakari, T. Suda, T. Kasai, T. Kumazawa, J. Onodera, H. Obara, *Tetrahedron* 61 (2005) 9630–9636.
- [24] S. Sato, H. Obara, A. Endo, J. Onodera, S. Matsuba, *Bull. Chem. Soc. Jpn.* 65 (1992) 2552–2554.
- [25] D.F. Eaton, *Pure Appl. Chem.* 60 (7) (1988) 1107–1114.